The Measurement of Trace Emissions and Combustion Characteristics for a Mass Fire

Ronald A. Susott, Darold E. Ward, Ronald E. Babbitt, and Don J. Latham

Concerns increase about the effects of emissions from biomass burning on global climate. While the burning of biomass constitutes a large fraction of world emissions, there are insufficient data on the combustion efficiency, emission factors, and trace gases produced in these fires, and on how these factors depend on the highly variable chemistry and burning condition of the fuel. Measurements made by satellites or aircraft can be used to estimate areas burned or ratios of specific emissions, but measurements close to the ground are needed to estimate actual amounts of fuel consumed, the rate of fuel consumption, and carbon and heat release by the fire. Ground measurements also provide information on changes in emissions as rapid flaming combustion passes, and burning is reduced to a much lower intensity smoldering phase of the fire—information that frequently gets integrated and lost by sampling from platforms at higher altitudes. The work reported here describes our development of a self-contained monitoring package specifically for use in high-intensity biomass fires and how it can be applied to numerous emission problems. In addition to understanding fire processes and fuel chemistry affecting the release of emissions, there is a fundamental need for a better understanding of fire dynamics of large fires (induced winds, heat release, turbulence, etc.). This information is needed to help solve problems associated with major wildfires.

The control of large fires remains a major concern to both the United States and Canadian governments. More than 2 million hectares (ha) of wild land burned in 1988, one of the worst fire seasons in recent times in the United States. Large fires such as the Canyon Fire in Montana burned over 100,000 ha in less than 24 hours—an incredible rate. Even though fire behavior associated with surface fires is reasonably well understood and predictable (Rothermel, 1972, 1983), models for predicting the behavior of mass fires and crown fires are not available (Albini, 1984). A better understanding is needed of fire behavior, spatial distribution of gaseous fuels, temperature profiles, and fluid motions within and adjacent to large fires. Feedback mechanisms resulting in rapid increases in the rate of heat release and rate of spread are poorly understood, as are mechanisms associated with the formation of emissions—especially emissions important from an atmospheric radiation transfer standpoint.

Results are presented of a continuing study of research that was started in 1988. A new sampling system was designed to provide fire dynamics data from within the fire. This chapter describes the sampling system, the measurements it provided on one biomass fire, and some valuable parameters that can be calculated such as emission factors, combustion efficiency, and rate of fuel consumption. The large prescribed fire in Ontario, Canada, provided a practical test of this package that can be used to assess the application of the monitoring concept to a broad range of biomass fires. Measurements of wind vectors, temperature, and emissions are reported for a 40-minute period from ignition through the critical period of maximum release of heat to the near extinction of the smoldering combustion phase.

Studies of large fires have included measurements of the concentration of CO, CO_2, and O_2 at or near street level between the piles of brush that simulated houses along streets (Countryman, 1964). Work completed by Hegg et al. (1989), Einfeldt (1989), and Ward and Hardy (1989) for the Lodi tests in California suggests emissions of graphitic carbon to be correlated positively with the rate of heat release. Emissions of chlorofluorocarbons, oxides of nitrogen, and lead may be related to the deposition of anthropogenically produced air pollutants. Ward and Hardy (1984) found that emission factors for total particulate matter without regard to size will increase with an increase in fire intensity, but emission factors for particles less than 2.5 μm mean mass cut-point diameter tend to decrease as the rate of heat release increases. Emission factors for particles less than 2.5 μm diameter, particles collected without regard to size, CH_4, CO, and CO_2 are all correlated with combustion efficiency (Ward and Hardy, 1990). Among other param-

Levine, J.S. (ed), 1991. Global Biomass Burning: Atmospheric, Climatic, and Biospheric Implications. Cambridge, MA: MIT Press.

eters, this study tested for nonstandard O_2 conditions on emissions production.

Experimental Methods

Selection of the Site and Fire Information

Hill Township near Chapleau, Ontario, was selected as the site for the prescribed burn (PB). The 490 ha PB was located about 30 km northwest of Chapleau and about 200 km north of Sault Ste. Marie, Ontario. This site was selected because of the uniformity of fuels and the relatively flat terrain. The site consisted of tramped fuels of white birch (*Betula papyrifera* Marsh.) and poplar (*Populus tremuloides* Michx.) with some jack pine (*Pinus banksiana* Lamb.) and black spruce (*Picea mariana* [Mill.] B.S.P.). The area had been three times treated with herbicides prior to the prescribed burn on 10 August 1989. Fuel loading as determined by Forestry Canada (McRae, 1989) for the unit was about 19.4 kg/m^2. The moisture content for fine fuels less than 0.5 cm in diameter averaged 23.3%, with the duff fuel top 2 cm averaging 43.6% and the lower layer 85.9%.

Weather associated with the Hill PB was influenced by a large area of high pressure in Illinois eastward through Ohio. Winds were generally less than 5 m/s and carried moist, warm air from the central region of high pressure to the north across Ontario. The dew-point temperature was about 14° to 15°C during the time of the Hill PB with a surface temperature of 26.0° to 26.9°C and relative humidity declining from 58% at 13:30 to 49% by 16:00. Surface winds were generally from the southwest at 3 to 4 m/s.

Our Fire Chemistry and Dynamics array of sensors and towers was in an area of intense study on the northwest side of the PB. A 25 m spacing was selected for the six towers with five of the towers placed in a pentagon around a central tower. Figure 32.1 shows the tower placement and scale, as well as the location of important site characteristics such as fuel wind rows, fuel breaks, and a road. Figure 32.1 also shows estimated fire front contours at selected times as the fire spread within the study area.

Equipment Development

Design of Fire Atmosphere Sampling System (FASS)

The operation of the FASS is controlled by a microprocessor-based computer designed for instrument applications. Special considerations in the design were portability, low power consumption, and ability to withstand exposure to the harsh fire environment.

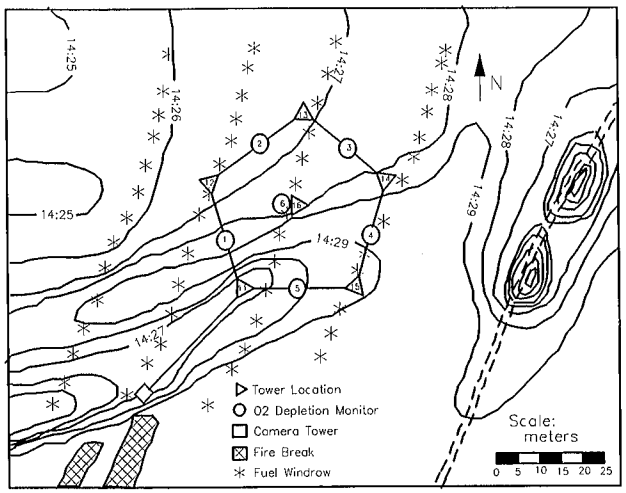

Figure 32.1 Pattern of fire spread through the matrix of towers from 14:25 to 14:30 hours on 10 August 1989.

The system collected information needed to characterize the atmosphere just above the flaming zone. This includes real time combustion gas concentrations, particulate matter production, and several fire dynamics parameters. The 40 kg packages of instruments were suspended, using standard television antenna towers, at a height of 12 m above the ground. The FASS network consisted of six systems deployed for the 1989 mass fire experiments. All systems started sampling simultaneously when signaled by a wire link connecting them that a fire was detected near the tower network.

Both glass fiber and Teflon filter mats were used to collect particulate matter during three consecutive periods (flaming, intermediate, and smoldering phases of the fire.) The FASS computer actuated valves to control the exposure sequence and combination of filters by combustion phase. Integrated samples of combustion gases were collected in sample bags for laboratory analysis. There were three bags for this purpose, one for each fire phase. Fire dynamics sensors consisted of wind and temperature measuring devices located on the tower (Figure 32.2). A three-dimensional wind measuring array, located on top of the tower (14 m), was constructed of three separate turbine type anemometers placed in an XYZ configuration. The vertical component of the air flow in the fire is used to calculate the flux of combustion products from the fire.

Methods for Real Time Measurements of CO_2, CO, and O_2 Combustion gases were drawn through filters by pumps for sampling particulate matter and the

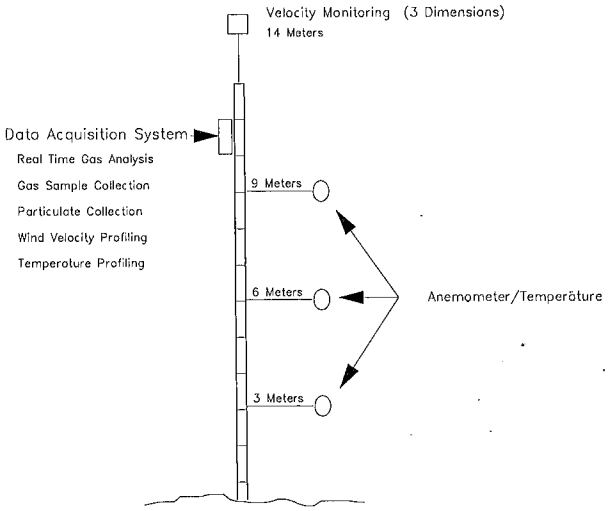

Figure 32.2 Position of the FASS sensors on the tower.

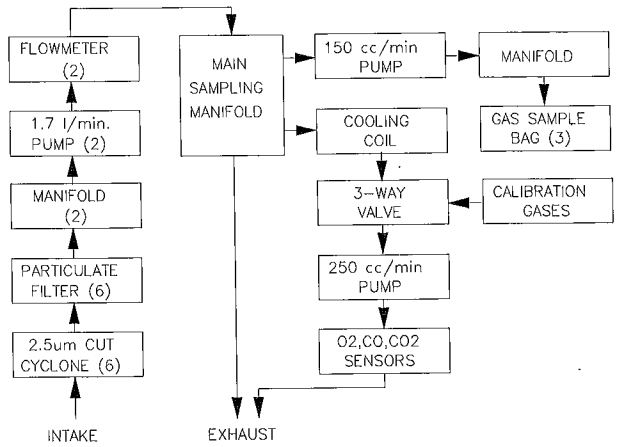

Figure 32.3 Diagram of the flow of the gases through the analyzers in the FASS packages.

filtered gases then analyzed for CO, CO_2, and O_2 (Figure 32.3). By minimizing volumes in the connecting tubing, the gas transit time between the external sample port and the sensors was kept to a few seconds. A valve also connected the sensor pump to a sample bag filled with calibration gas (CO_2 at 7310 parts per million, ppm, and CO at 500 ppm in air) to provide a check of the sensor span during the fire. The O_2 sensors were G. C. Industries Inc.[1] model 33–270 electrolytic cells, designed to measure O_2 in gas mixtures with CO_2 concentrations up to 20%. O_2 sensor accuracy was specified to be 2% of full scale (or 0.5% O_2) at constant temperature, and 5% of full scale over the range of 0° to 50°C. The CO sensors were also electrolytic cells manufactured by G. C. Industries Inc. (model 44–300). Linearity was specified to be 1%, and accuracy depended on the CO concentration accuracy of a calibration gas mixture. The CO_2 sensors were nondispersive infrared gas monitors manufactured by Valtronics (Model 2015 BMC). Accuracy was specified to be within 3% of full scale. The three gas sensors were calibrated by standard gases with certified composition and zero grade air.

Wind Sensors Triaxial wind speed was measured by three turbine anemometers manufactured by Qualimetrics (model 24201). Calibration of one of these anemometers in the Intermountain Fire Sciences Laboratory (IFSL) wind tunnel was used for all 18 anemometers placed in the Hill PB. Wind speed accuracy is expected to be within about 0.25 m/s.

Thermocouples All thermocouples exposed to the fire environment were constructed of 24 gauge type K (chromel/alumel) wire protected by a braided stainless-steel sheath. Thermocouples within the sample packages were 30 gauge with a glass fiber sheath. Temperature accuracy is expected to be within 4°C from 0° to 400°C, with larger errors at higher temperatures.

Sampling Protocol

The system computer timed and controlled data acquisition events during the experiment. In general, the objective was to maximize the data collected during the 40 minutes following fire detection near the tower array. It was also necessary to record baseline data (at a lower sampling rate) prior to the fire as well as smoldering data for several hours after the fire front had passed. All computer clocks were set to real time (EDT) based on the Hill PB experimental clock.

Real Time Sensors On the day of the burn, the FASS was programmed to first calibrate the gas sensors at 12:00. From this time on the FASS could accept a trigger from a temperature-activated fire sensor. Every two minutes the program made a reading of background (no fire) data. These data provided an ambient air measurement for the gas sensors, prefire wind speed and direction, and air temperatures. The approaching fire was detected when a ground temperature sensor exceeded 67°C. These sensors were placed in piles of fuel up to 30 m west of the tower array, in the direction anticipated for fire arrival. All

[1]The use of trade or firm names in this chapter is for reader information and does not imply endorsement by the U.S. Department of Agriculture of any product or service.

FASS packages were linked and began real time measurements (two readings per second) when the fire was detected. The next 40 minutes were viewed as three fire phases: a 10-minute flaming phase, a 10-minute intermediate phase, and a 20-minute smoldering phase. A second calibration was made at the start of the smoldering phase to reduce the effects of sensor drift. Finally, the packages returned to taking one reading every two minutes, as in the prefire sampling phase. This extended smoldering phase continued until the tower package was turned off, or storage memory was full.

Integrated Filter and Gas Bag Samples The tower packages collected physical samples during three of the sampling phases, for later analysis. Particulate matter was collected for flaming, intermediate, and smoldering phases. Three gas sample bags were also filled in each tower package over the same time intervals as the three filter particulate samples.

Analytical Methods for Postfire Sample Analysis

The gas sample bags from the Hill PB were analyzed for CO_2 and CO composition using infrared gas analyzers (Horiba model PIR-2000). Bags of zero air and a span gas mixture were also analyzed to adjust the instrument to zero and to calculate bag composition. The accuracy of this method is about ± 1% composition for both CO_2 and CO.

The membrane and glass fiber filters were weighed at IFSL to determine smoke particle loading. Filters were conditioned at 50% relative humidity and 22°C for 24 hours for initial and final weighing on a Cahn model C-32 microbalance. Filter blanks were within 0.010 mg before and after the experiment. Membrane filters were also analyzed for trace metals using an X-ray fluorescence method at NEA Inc. of Beaverton, Oregon. The glass fiber filters were analyzed for graphitic and organic carbon fractions by Sunset Laboratories, using a ramped temperature protocol for carefully volatilizing the organic carbon fraction while retaining the graphitic carbon fraction.

Calculated Parameters and Methods of Adjusting Data

Emission factors were calculated using the carbon mass-balance method (Ward et al., 1979; Radke et al., 1990). The method is based on the partial oxidation of fuel (typically $C_6H_9O_4$) to CO_2 and products of incomplete combustion. The assumption was made that the carbon is released from the fuel proportional to the mass-loss rate of the fuel consumed by the fire. This assumption was validated for laboratory fires by Nelson (1982). For each gram of carbon released, approximately 2 grams of $C_6H_9O_4$ are consumed. By accounting for the carbon contained with the CO_2, CO, hydrocarbons, and particulate matter, the equivalent amount of fuel consumed can be evaluated. (In practice, the CO_2 and CO account for 95% to 99% of the carbon released from the fuel.)

An emission factor is computed by dividing the concentration of the emission (g/m^3) by twice the total carbon concentration (g/m^3). The FASS units were specifically designed to make the measurements needed by phase of combustion so that these calculations could be made for the flaming, intermediate, and smoldering combustion phases. In the case of particulate matter, the concentration was computed by averaging the mass of particulate matter collected on the glass fiber and Teflon filter mats and dividing this by the average volume of gas sampled.

Rate of fuel consumption calculations were made as in Ward and Hardy (1984) by multiplying the carbon concentration as measured using the CO_2 and CO real-time sensors (g/m^3) by the vertical component of smoke plume velocity (m/s), and the resulting number by two (accounts for the molar ratio of fuel to carbon). The error associated with not measuring the particulate matter and hydrocarbons in real time is less than 5%. Individual source strengths for emissions can be calculated by multiplying the concentration (g/m^3) by the vertical velocity (m/s).

The rate of heat release was computed by multiplying the rate of fuel consumption by the fuel heat of combustion corrected for the heat remaining in the products of incomplete combustion. The real time CO concentration was the only significant emission resulting from incomplete combustion and was used in making the adjustment to the heat of combustion. Based on oxygen bomb calorimeter measurements of the heat of combustion, a value of 20 kilojoules per gram (kJ/g) was selected (McRae, 1989) and 10.1 kJ/g was used for CO (Perry and Chilton, 1973). The resulting rates of heat release driving the convection column were not corrected for other forms of heat loss due to radiation and soil heating.

Presentation of Data

In this section, the general fire behavior and deviations from ambient conditions for each of the measured parameters are discussed. Because this was the first full-scale deployment of the FASS system, the performance of the sampling system is discussed. Concentration of combustion products and the "nor-

malcy" of the data are presented. Comparisons are made of the concentrations of various combustion gases and the multiple measurements of these gases through grab sampling and real time techniques. General observations of the wind field parameters are presented.

Fire Behavior

The area of the fire ignited surrounding the FASS array was 97 ha. Ignition of this block commenced at 14:19 hours with approximately 8 ha involved by 14:23 hours. At 14:22 hours, a line of fire was ignited 50 m to the east of the array of towers (Figure 32.1). Approximately two minutes later, three segments of fire were ignited 60 m to the west of the tower array, and this line of fire terminated at the fire break test site just to the south. By 14:25:44, the fire had advanced from the central segment of fire to within 25 m of the base of FASS package tower 12. The triggering mechanism was activated in this location and the six FASS packages simultaneously began sampling the environmental parameters.

Fuels were distributed across the tower array nonuniformly. Wind rows of concentrated heavy fuels, resulting from the cable clearing of the area, extended north-northeast, and FASS tower 12 was on the easterly edge of one of these wind rows. FASS towers 16 and 13 were in a second wind row with a third wind row passing just to the east of FASS towers 14 and 15. The center lines of each of the three wind rows of heavy slash are shown by the lines of asterisks in Figure 32.1. The fire spreads along these wind rows more rapidly than between the wind rows so that the spread pattern actually tended to follow the wind rows and seemed to move forward from wind row to wind row in pulsing actions. Potentially, some of the pulsing periodicity of the fire could have been associated, on a micro scale, with the spread of the fire between wind rows of fuel.

The rate of spread of the fire from the line of ignition to the trigger location was calculated to be about 0.5 m/s. Flame lengths were on the order of 8 to 15 m based on video coverage of the burn area and from photographs taken from a helicopter observation point. The main fire front flanked along a line extending from FASS towers 12 to 13 toward FASS tower 16 in the middle of the sample array while a finger of fire was running through the array from FASS tower 11 toward FASS tower 15. The north flank of the finger along a line from FASS 11 to FASS 15 and the southerly flank spreading southward from FASS 12 and FASS 13 converged in the vicinity of FASS packages 16 at approximately 14:29:00, or about 4.25 minutes after the FASS packages were activated.

The flame burnout time for the fire was on the order of one to three minutes depending on the location in or between wind rows. This affected the duration of the flaming phase emissions production at all of the FASS package locations.

There were three major convergence zones associated with the fire ignition pattern for block A that could have affected the measured patterns of airflow in the vicinity of the FASS packages.

1. The first of these occurred during the time that the center fire was converging to the east of the FASS array. This was believed to occur during the period from 14:26 to 14:30.
2. The second occurred soon after ignition of the area to the west of the fire break test area during the time that the lines of fire were converging at approximately 14:34.
3. The third occurred during the time that major segments of the fire on the southwestern flank of the block were converging to the south and slightly to the east of the FASS array.

The ignition of the 97 ha block was completed by 14:55.

Gas Concentrations

The concentrations of the primary gases needed for carbon mass balance calculations and emission factors were available from analyses of gas collected in sampling bags and the measurements of the real time sensors. Table 32.1 contains the results of the sample bag analysis for CO_2 and CO, by sampling phase. CO_2 is highest for the flaming phase, with the highest level measured for package number 14, at 4490 ppm. Inter-

Table 32.1 FASS sample bag gas concentrations in ppm

Box number	Flaming		Intermediate		Smoldering	
	CO_2	CO	CO_2	CO	CO_2	CO
11	3217	126	1937	152	1305	172
12	3420	142	1751	120	1353	164
13	4166	168	1969	175	1224	151
14	4490	154	2140	198	1264	170
15	3963	137	a	a	1248	170
16	3922	140	1961	174	1321	172
Average	3863	144	1951	164	1286	167

a. Valve did not open.

mediate phase values drop to about 50% of the flaming value, and the lowest levels (1224 ppm) occur during the smoldering phase on package 13. CO_2 levels were quite uniform across the sample array with deviations from the average of about 11% during flaming and only 3% during smoldering. Trends in CO concentrations with fire phase are less obvious, and these values tend to be uniformly between 120 and 200 ppm. Flaming phase CO averaged about 12% lower than the later phases, but the data are not consistent.

Continuous CO_2 and CO measurements were made during the three fire phases. The background concentrations of CO_2 and CO in air can be assumed to be 375 and 1 ppm, respectively. The average of the concentration curve over the time assigned to a phase should be equal to the sample bag concentration. Figure 32.4 shows the real time sensor concentrations for FASS package 11. The CO_2 levels in Figure 32.4a show the high variability of these levels, from near ambient levels to 9000 ppmv during the 10 minutes of the flaming phase. The rapid response of the CO sensor (Figure 32.4b) emphasizes the variability even more. Comparison of Figures 32.4a and 32.4b in the first 200 to 300 seconds of flaming show the high efficiency of the initial flaming pulse, with little CO produced. The CO concentrations increase relative to CO_2 as the fire goes to the smoldering phase. The nearly constant region at about 14:46:40 is due to switching a flow of calibration gas to the sensors.

Table 32.2 provides a summary of real-time sensor results for all FASS packages, by phase of combustion. The second smoldering phase data were taken from the two hours of sampling following the initial 40 minutes of the fire. Figure 32.5 shows a comparison of average CO_2 and CO as a scatter plot of the real time results versus the sample bag measurements. Clearly, there is good agreement between the two methods. A linear regression of the CO_2 data gave a slope of 1.17

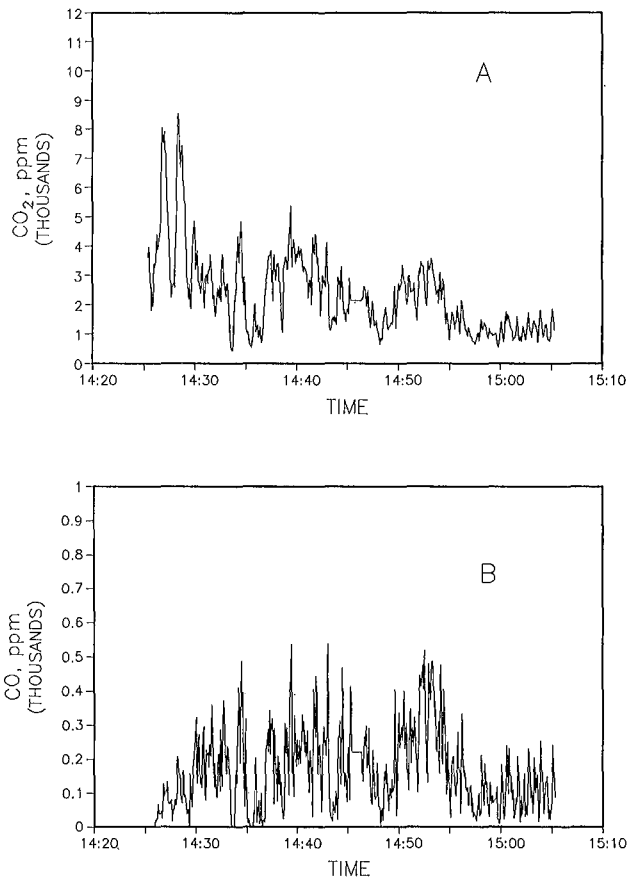

Figure 32.4 Example of real-time gas concentration measurements on FASS 11: (a) CO_2; (b) CO.

Table 32.2 FASS real-time combustion gas sensor summary

Box number	CO_2 (ppm)		CO (ppm)	
	Average	Maximum	Average	Maximum
Flaming phase (10 minutes)				
11	3518	8616	136	515
12	3595	11551	123	500
13	4737	12536	169	523
14	5467	11995	137	442
15	4772	12660	125	394
16	3848	8370	132	637
Average	4323	10955	137	502
Intermediate phase (10 minutes)				
11	2623	5604	189	767
12	2322	5233	128	664
13	2683	5798	170	648
14	2709	6602	161	545
15	3162	5219	197	468
16	2272	5514	155	808
Average	2629	5662	167	650
Smoldering phase 1 (20 minutes)				
11	1648	4666	163	595
12	1763	4659	173	493
13	1786	4501	164	555
14	1757	4889	157	524
15	1688	4772	165	577
16	1759	4628	161	839
Average	1734	4686	164	597
Smoldering phase 2 (2 hours)				
11	722	1830	40	222
12	641	1201	61	169
13	729	1313	52	159
14	717	1259	47	130
15	613	1409	64	115
16	830	1252	37	134
Average	709	1377	50	155

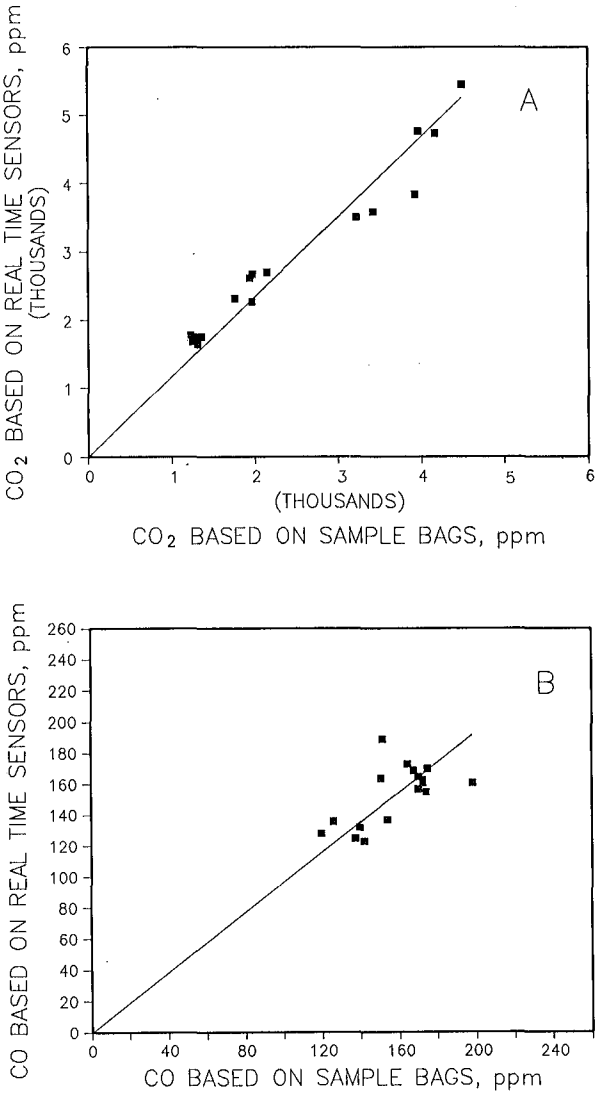

Figure 32.5 Comparison of the average real-time gas concentrations with measurements based on sample bags: (a) CO_2; (b) CO.

with $r^2 = 0.93$ (the intercept is forced to zero). The high slope is attributed to remaining difficulties in calibrating the sensor and a slight decrease in bag CO_2 due to leaky valves. A plot of the CO data (in Figure 32.5b) gave a linear regression line slope of 0.966 with $r^2 = 0.28$. The relatively small range of concentrations measured leads to the poor fit, but the two methods give comparable concentrations. The agreement should improve as we improve the real time sensor calibration methods. Relative differences of 3% to 5% should be possible in future experiments.

Oxygen levels were measured in real time by the tower-mounted systems. The data show early flaming phase minima of about 90% to 92% of air level, or a decrease of about 0.02 volume fraction. Some broad decreases in O_2 level were seen in later-phase curves, but most of the detail was lost in noise and drift of the sensor. The O_2 sensors should be improved in resolution or accuracy for this application on relatively dilute combustion gases.

Particulate Matter Concentrations

The tower packages collected particulate matter by fire phase on two filter media (glass fiber and Teflon). Table 32.3 gives particulate matter concentrations by fire phase. The concentrations ranged from 15.1 to 39.9 mg/m^3. These values are about five to 10 times lower than those of CO, and therefore make a smaller contribution to the carbon balance and combustion efficiency calculations. All packages were within about 25% of the average value for a phase. The smoldering phase has slightly higher concentrations and produces more total particulate matter in the 20-minute sampling. The average for the two filter media was used to calculate emission factors for PM5.0.

The glass fiber filters were analyzed for carbon content, proportioned between graphitic and organic carbon. The organic carbon percentage averaged lowest for the flaming phase (45.5%) and increased at later times (52.1% for intermediate and 53.6% for the smoldering phase). There is considerable variation during the flaming phase, reflecting the highly turbulent fire and entrainment of ash and soil particles. Graphitic carbon averaged 8.1% during the flaming phase and decreased dramatically in the intermediate (2.9%) and smoldering (1.5%) phases. The intermediate phase results are closer to those for the smoldering phase. Low graphitic carbon during the intermediate phase indicates a substantial decrease in flaming combustion. The total percentage carbon in the fine particles is approximately equal (53.5% to 55.1%) for all three fire phases.

The Teflon filters were analyzed for trace inorganic elements. Figure 32.6 shows a comparison of the Hill PB elemental profile to those from experimental burns in California and the Pacific Northwest. The calcium levels were high compared to other reports and are probably due to the soil chemistry at the burn site. Considerable levels of elements from aluminum to calcium were measured, along with manganese, iron, and zinc. Although there is considerable variation between tower boxes, the S, Cl, and K are highest during flaming, while Al, Si, Ca, and Fe tend to increase in the smoldering phases. These results are consistent with other studies.

Table 32.3 FASS filter particulate (PM 5.0) concentrations (mg/m^3)

Box number	Flaming		Intermediate		Smoldering	
	Glass	Teflon	Glass	Teflon	Glass	Teflon
11	24.5	28.9	39.9	24.8	36.1	24.6
12	21.2	15.1	19.5	15.8	28.7	25.6
13	29.1	26.2	26.7	23.3	27.4	24.5
14	28.8	24.9	26.5	24.0	27.0	25.2
15	28.7	28.5	a	a	30.4	28.2
16	32.1	18.3	23.7	21.1	28.9	25.8
Average	27.4	23.6	27.3	21.8	29.8	25.7

a. Valve did not open.

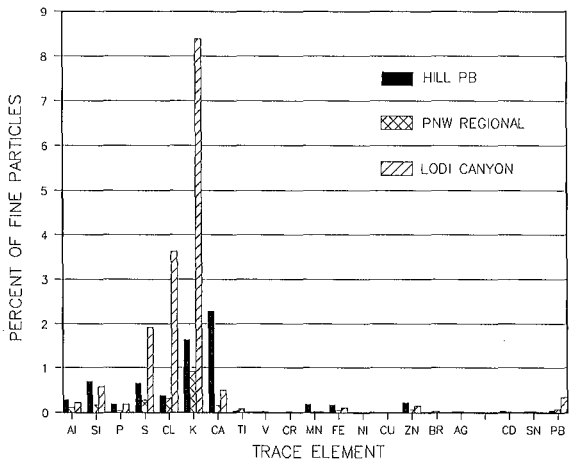

Figure 32.6 Inorganic composition of particulate matter compared to literature values for Pacific Northwest and Lodi Canyon, California, burns.

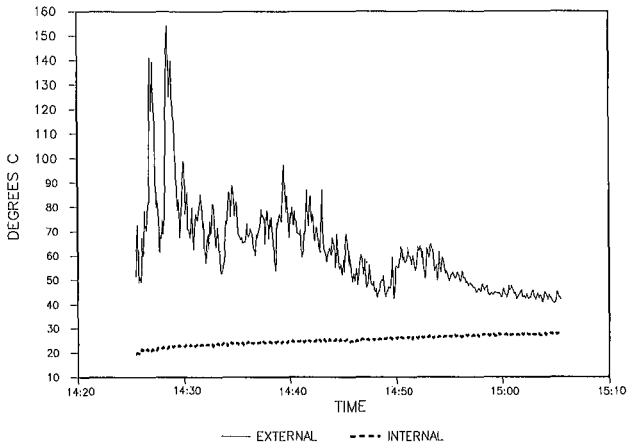

Figure 32.7 Comparison of the FASS 11 internal gas flow temperature to the external air temperature of the fire environment.

Temperature Measurements

Survival of the sensitive instruments in a harsh fire environment requires the internal temperatures to remain close to ambient. Thermal protection of the FASS depended on a low-density ceramic insulation and a highly reflective aluminum outer wrap. Figure 32.7 compares the internal gas flow temperature to the external fire environment temperature at the inlet, for FASS 11. While the outside temperatures reached over 150°C, the internal box temperatures increased only about 10°C. FASS 12 was exposed to air temperatures as high as 450°C, but average temperatures for the flaming phase ranged from 80° to 137°C. There was no damage to any of the FASS packages. The modest internal temperature changes suggest that the system designs can withstand much more severe fires.

Wind Speed and Direction

Wind speeds were measured in three dimensions by the set of turbine anemometers positioned above the FASS, at the top of the tower. The positive or negative direction sensors on these anemometers failed but the absolute values of the vector wind speeds were reliable. Other data indicate that the wind was always from the west and predominately slightly south of west. These results were consistent with other horizontal wind direction measuring systems located at the same tower locations.

Vertical wind directions should be mostly up, due to buoyancy of the hot combustion gases. The vertical component of wind velocity varied rapidly from 0 to over 6 m/s for brief peaks but averaged between 2 and 3 m/s for most of the fire. Generally, we expected the temperature and CO_2 concentrations to be correlated with the vertical velocity of the combustion gases. In

fact, this was found to be a valid correlation and for the FASS tower location, we found no evidence during the flaming and intermediate sampling periods for significant down drafts. On occasion, the concentration of excess CO_2 dropped to near zero, and the vertical velocity was also near zero. We concluded that the errors in calculating the rate of fuel consumption and the rate of heat release from the carbon mass balance considerations would be minimal. The vertical velocity was used in conjunction with the real time gas sensors to calculate the mass flux of carbon from the fire site.

Discussion

In this section, we discuss the findings from the FASS data set. The rate of fuel consumption is used in evaluating the rate of emissions production for the fire over time as well as the total rate of heat release corrected for combustion efficiency. The emission factors are presented by combustion phase and weighted for the entire fire.

Rate of Fuel Consumption

The rate of fuel consumption is important for calculating source strength and the rate of heat release over the life history of the fire. Here we use the data from the vertical wind velocity, CO concentration, and CO_2 concentration to calculate the rate of release of carbon from the biomass fuel. Four of the six FASS packages yielded satisfactory data for calculating rate of fuel consumption (FASS packages 11, 12, 14, and 16). The integrated fuel consumption is compared with the fuel inventory measurements of total fuel consumption by Forestry Canada (McRae, 1989).

Elemental carbon composition of the fuels is important to the accuracy of carbon mass balance methods. Fuels typical of those burned during the Hill PB were collected by Forestry Canada and shipped to the IFSL. Table 32.4 provides a list of the species and size ranges analyzed, along with the elemental composition of the fuel (C, H, N, and O estimated by difference). The moisture and ash component available from thermogravimetric analysis were used to reduce composition values to an ash-free, moisture-free basis. This basis allows easier comparison of just the organic component of the forest fuels. The woody component is the largest fraction of the fuel, and the carbon fraction of the woody material approaches 50%.

Generally ash is low (0.5% to 1%) in the woody material but is up to 7% of black spruce twigs. The

Table 32.4 Elemental analysis of Canadian fuels from the 1988 mass burn

Sample identification	C(%)	H(%)	N(%)	O(%)
Timmins duff	58.19	5.29	1.82	34.70
Timmins litter	57.54	6.33	1.26	34.87
White birch twig (0.0–0.49 cm)	54.39	6.30	0.85	38.47
White birch wood (3.0–4.99 cm)	49.86	6.01	0.10	44.03
White birch wood (7.0+ cm)	49.50	6.07	0.09	44.33
White birch bark (3.0–4.99 cm)	57.82	6.82	0.47	34.89
White birch bark (7.0+ cm)	58.74	7.08	0.49	33.69
Black spruce twig (0.0–0.49 cm)	56.45	6.37	0.61	36.57
Black spruce wood (3.0–4.99 cm)	52.02	6.10	0.18	41.70
Black spruce wood (7.0+ cm)	50.59	6.05	0.05	43.31
Black spruce bark (3.0–4.99 cm)	57.92	6.06	0.48	35.54
Black spruce bark (7.0+ cm)	53.34	5.77	0.29	40.60
Jack pine twig (0.0–0.49 cm)	55.03	6.26	0.57	38.13
Jack pine wood (3.0–4.99 cm)	51.38	5.97	0.05	42.60
Jack pine wood (7.0+ cm)	51.37	6.15	0.04	42.43
Jack pine bark (3.0–4.99 cm)	52.31	5.91	0.48	41.30
Jack pine bark (7.0+ cm)	54.34	5.92	0.24	39.50
Poplar twig (0.0–0.49 cm)	56.52	6.60	1.06	35.82
Poplar wood (3.0–4.99 cm)	50.71	6.09	0.15	43.05
Poplar wood (7.0+ cm)	49.25	6.07	0.05	44.63
Poplar bark (3.0–4.99 cm)	54.80	6.54	0.82	37.84
Poplar bark (7.0+ cm)	52.75	6.33	0.40	40.52

Note: Compositions are on a dry weight and an ash-free basis.

duff and litter samples have 10% to 20% ash. This ash component should be investigated in more detail as a source of potential hazardous emission or as a useful tracer for smoke from biomass burning. Because oxygen is the only other major component it can be estimated by difference. The propensity for soot or particulate matter emissions to form may be indicated by the oxygen content, which covers a range of 33.7% to 44.6% for the Canadian samples. Soot formation is expected to increase with lower oxygen content, making the white birch bark an important source of soot.

Measured Rate of Fuel Consumption The peak rate of fuel consumption occurred during the time when the fine fuels were consumed by the advancing fire. Peak rates of fuel consumption were measured at 40.8, 64.5, 61.4, and 36.1 $g/m^2/s$ for packages 11, 12, 14, and 16, respectively. Figure 32.1 shows the time of ignition for the fuel immediately surrounding each tower location. The maximum rate of fuel consumption occurred at an elapsed time from triggering of the FASS sample packages of 2.83, 1.00, 4.33, 2.5, and 4.33 minutes for packages 11, 12, 14, 16A, and 16B, respectively. (For FASS package 16, two peaks of fuel consumption were measured and are identified as 16A and 16B.) From Figure 32.1, the wind rows adjacent to and upwind from FASS towers 12 and 14 contributed to the high rates of fuel consumption. In addition to a wind row being immediately upwind of FASS tower 16, the fire converged immediately under FASS tower 16 and probably contributed to both the sustained high rate of fuel consumption and the double peak phenomena observed for the rate of fuel consumption.

The ambient winds were substantial, averaging 3.1 m/s at 14:00 (McRae, 1989), immediately prior to ignition of block A of the Hill PB. Undoubtedly, smoke drifted into the region of flux measurements because the fire was ignited in steps starting with the center fire and extending out past the FASS array in an ever increasing circle. This could have influenced the measurements more during the smoldering phase than during the initial ignition phase. It is likely that some of the emissions created in the vicinity of the FASS packages exited the area without being accounted for through the carbon mass-balance and flux measurements. The overall significance is not known but is thought to be no greater than the level of error associated with the fuel consumption measurements.

Total Fuel Consumption Total fuel consumption for each of the four sets of measurements was calculated by integrating the rate of consumption. The cumulative fuel consumption over time is shown in Figure 32.8. Total fuel consumption averaged 11.46 kg/m^2 with a standard deviation of 1.65 kg/m^2. The range of fuel consumption of 9.76 to 13.61 kg/m^2 coincides with the areas of total fuel loading (Figure 32.1). The rate of fuel consumption was still decreasing at the end of the sample period and averaged 1.06 $g/m^2/s$ after 40 minutes of sampling. The fuel consumption rate continues to be significant through the end of the smoldering sample period. Figure 32.8 shows a steep rate of fuel consumption over the first four to six minutes following ignition, during the time when the fine fuel component is consumed.

The FASS data allow calculation of fuel consumption for the flaming, intermediate, and smoldering combustion periods by integrating the rate of fuel consumption curves over the limits of integration for those periods (Table 32.5). The average total fuel consumption of 11.46 kg/m^2 compares with the inventory value from data collected by Forestry Canada of

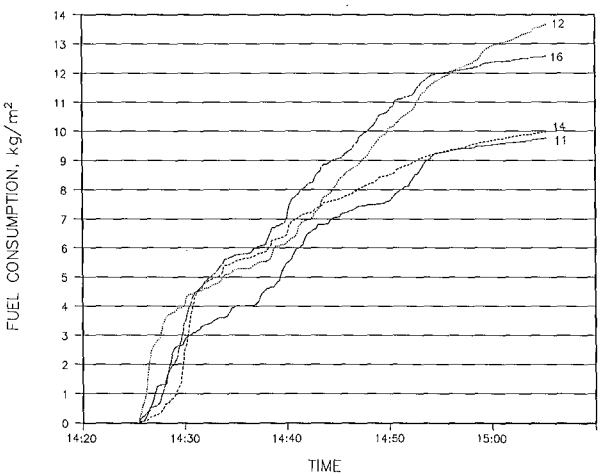

Figure 32.8 Cumulative fuel consumption for each of the four sets of data (packages 11, 12, 14, and 16) for Hill PB.

Table 32.5 Fuel consumption by phase of combustion and the total, for each of the four FASS packages (kg/m^2)

FASS number	Flaming	Intermediate	Smoldering	Total
11	4.00	3.17	2.57	9.76
12	5.24	3.13	5.24	13.61
14	5.58	2.12	2.26	9.96
16	5.73	3.35	3.45	12.53
Average	5.14 ±0.68	2.94 ±0.48	3.38 ±1.16	11.46 ±1.65

10.63 kg/m^2 or about 8% greater than the ground inventory. Examining the fuel consumed for the first six minutes for each FASS package yields measured fuel consumption averaging 4.22 kg/m^2. This is about twice the fine fuel loading on the unit. However, an additional component of fuel including a portion of the duff and larger-diameter fuel fractions was consumed during the flaming phase.

An approximate mathematical expression was fit to the rate of fuel consumption data to simplify other source strength and heat release calculations for the entire area of the Hill PB. More rigorous modeling of the fuel consumption process is beyond the scope of this report. Ward and Hardy (1984, 1989) modeled the rate of fuel consumption using a similar set of carbon flux data for broadcast burns of logging slash on clear-cut units in Oregon and Washington. They used an equation that provides for an exponential growth and decay of the combustion process. We use a linear growth function to describe the buildup phase and an exponential decay function for the diedown phase.

The four sets of data for the rate of fuel consumption were averaged (Figure 32.9). The maximum rate of fuel consumption was approximately 20 g/m^2/s (corresponding to a relative rate of 1.0 in Figure 32.9), which occurred 4.5 minutes after the sensors were first challenged by the approaching fire. A linear fit with a slope of 0.074 g/m^2/s/s was used for the buildup phase. The diedown phase uses an exponential decay function stretched over two hours with a time-decay constant of 10 minutes. The resulting model lines for growth and decay are also shown in Figure 32.9. The exponential decay function gave a reasonably good fit for the period from 12 minutes to the end of the sampling period. In addition, because of the indicated high rate of fuel consumption sustained at the end of the sampling period, the model was extended for another 80 minutes. While details of the model are not exact due to ignition pattern, fuel concentrations, and ambient winds, the model does give a good representation of the average trend in burning rate with time. The model fuel consumption values are easily calculated for any time interval and can be used to compute the source strength for particulate matter, CO, CO_2, and other compounds as a function of the rate of ignition for the unit.

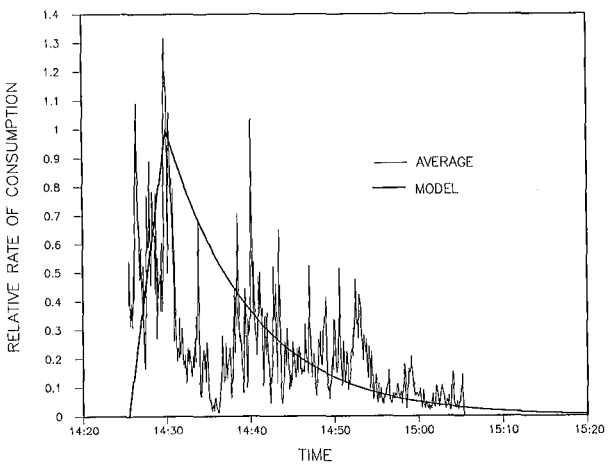

Figure 32.9 Fit of a simple model to the average rate of fuel consumption.

Emission Factors and Emissions Released Per Unit Area Burned

Figure 32.10a shows the average CO emission factors compared to results from fires in Douglas fir and

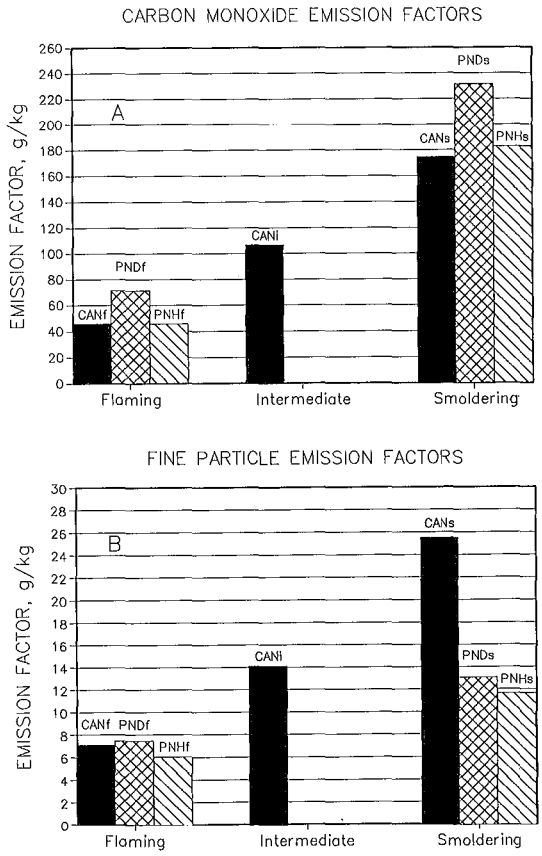

Figure 32.10 Comparison of emission factors measured for the Hill PB Canada (CAN) with data from Pacific Northwest Douglas fir (PND) and Pacific Northwest hardwood (PNH): (a) CO; (b) PM 5.0. Flaming, intermediate, and smoldering phases are indicated by *f, i, s*.

hardwood slash in the Pacific Northwest. There is excellent agreement with the hardwood slash, but the Hill PB has somewhat lower CO emission factors than for Douglas fir slash. Emission factors for CO increased from 46 g/kg during flaming to 174 g/kg during smoldering. Combustion efficiency decreased from 95% for flaming to 82% for smoldering as a result of the increased emission of incompletely oxidized combustion products.

Figure 32.10b shows the average fine particle emission factors from the Canada fuels compared to the Northwest United States fuels. There is good agreement during the flaming phase, but emission factors for PM 5.0 during the smoldering combustion phase for the Canada fuels are about twice those for the United States fuels. The average PM 5.0 increased from 7.17 g/kg during flaming to 25.6 g/kg during smoldering.

Emission factors are weighted based on the fuel consumed during each of the sampling periods for the flaming, intermediate, and smoldering combustion phases of 5.14, 2.94, and 3.38 kg/m^2, respectively. The emission factor data shown in Figure 32.10 for each sampling period is multiplied by this fuel consumed during the sampling period to give the total emissions by phase in Table 32.6. The totals in this table represent the total emissions produced by the fire on a square meter basis.

The total emissions released per square meter of area burned were 165, 1141, and 18,887 g/m^2 for PM 5.0, CO, and CO_2, respectively, based on our measured fuel consumption. By dividing the total emissions by the total fuel consumed (11.46 kg/m^2), fire-weighted emission factors are calculated for the Hill PB of 14.4, 99.6, and 1648 g/kg for PM 5.0, CO, and CO_2, respectively.

Application of Unit Area of Measurement to the Hill Fire

The total emissions released from the Hill PB can be calculated based on the fuel consumption and the fire-weighted emission factors. The total area burned of 390 ha multiplied by the emissions released per square meter yields a total emissions production of 643, 4450, and 73,700 tons of PM 5.0, CO, and CO_2 for the Hill PB. Block A, the area of the intensive fire chemistry and dynamics study (97 ha), released about 25% of the emissions of the total Hill PB.

Table 32.6 Total emissions released on a g/m^2 basis for block A of the Hill PB

Emission	Flaming	Intermediate	Smoldering	Total
PM 5.0	36.9	41.6	86.4	164.9
CO	236.4	313.7	590.5	1141
CO_2	8980	4813	5094	18,887

A source strength calculation requires information pertaining to the rate of ignition of the fuels and the rate of consumption during the burnout time for the fuels. The mathematical expressions for the rate of fuel consumption can be applied here, along with emission factors for the individual phase of the fire. The rate of ignition is not known accurately, but we estimate the helitorch and advancing fire ignited new area at a steady state of about 350 m^2/s 20 minutes after starting the center fire. Ignition of new area stopped about 50 minutes into the fire, and remaining fires burned together 10 minutes later. Figure 32.11 shows how this ignition pattern would generate fine particulate matter from block A of the Hill fire. The flaming phase produces most of the particles in the first 20 minutes, but smoldering dominates for the remainder of the fire. Other emissions can be computed accordingly. Maximum rates of production of PM 5.0, CO, and CO_2 are estimated as 0.047, 0.33, and 6.3 tons per second.

The FASS-measured CO production allows the calculation of an effective heat of combustion as the fuel is consumed. For example, if 10% of the original fuel carbon is converted to CO, the heat of combustion of that CO can be subtracted from the heat expected from the total fuel burned (20 kJ/g). Other products of combustion can be ignored as a first order approximation. The overall average heat of combustion was

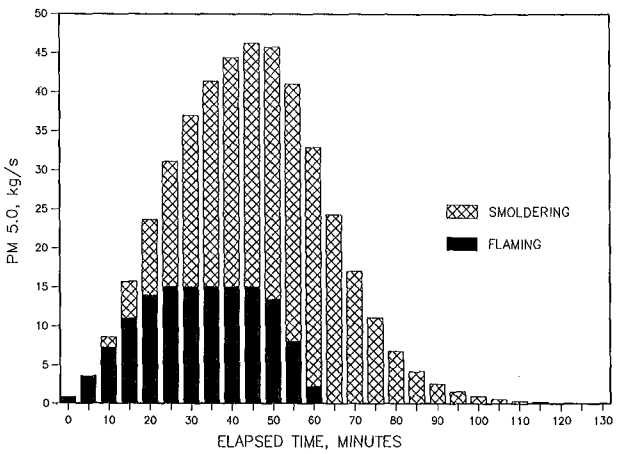

Figure 32.11 Source strength over time for particles less than 5.0 micrometers.

calculated to be 19.22 kJ/g, or about 96% of the total. This value changes slightly with phase of combustion as combustion efficiency changes. Peak heat release rates of about 500 kW/m^2 were calculated about five minutes after the fire reached the FASS array. The estimates of ignition rates in the previous paragraph result in a 75,000 megawatt (MW) heat release rate for the entire block A of the Hill PB. Some of this heat is lost to soil heating or is radiated away, but a majority heats the surrounding air and smoke to provide the driving force to build the strong convection column.

Summary and Conclusions

The Fire Atmosphere Sampling System (FASS) has been tested within an intense mass fire without major problems. The measurements and samples taken provide detailed information on emissions within the fire. Continuous measurements during a fire can provide needed insight on the flaming and smoldering of large fires, and temporal variations of emissions. The vertical measurements of air flow, combined with the concentrations of CO_2 and CO, accurately calculate the mass flux of carbon released. The measured fuel consumption based on the carbon mass flux agreed with ground inventory methods. These inventory methods are not possible in fuels common to global biomass burning, where the FASS can be easily applied. The detailed fuel consumption rate allows more realistic and accurate models of the local burning process to be developed.

The computer system incorporated in the FASS allows numerous possibilities for modifications to meet alternate needs. Emphasis in the current system was on release of carbon and the nature of particulate matter, but additions could easily be made to measure nitrogen gases or other greenhouse and hazardous emissions. The self-contained system can easily be transported to fires throughout the world to provide a ground truth addition to remote sensing studies.

Acknowledgments

The efforts of many groups and individuals aided the development, construction, and deployment of our experiment—we gratefully acknowledge their contributions. The fire research personnel of Forestry Canada, Ontario Region, provided needed support in site selection, fuels characterization, and tower assembly and were gracious hosts during our visit to Canada. Of special recognition are the space, accommodations, telephone, facsimile, and aircraft support provided by the Ontario Ministry of Natural Resources. This research was supported in part by funds provided by the Defense Nuclear Agency under project IACRO 89-903, Task RA, Work Unit 00024.

REFERENCES

Albini, F. A., Wildland fires, *American Scientist*, 72:590-597, 1984.

Albini, F. A., Thermochemical properties of flame gases from fine wildland fuels, *Res. Pap. INT-243*, Ogden, UT: U.S. Department of Agriculture, Forest Service, Intermountain Forest and Range Experiment Station, 42 pp, 1980.

Countryman, C. M., Mass fires and fire behavior, *Res. Paper PSW-19* Berkeley, CA: U.S. Department of Agriculture, Forest Service, Pacific Southwest Forest & Range Experiment Station. 53 pp, 1964.

Einfeldt, W., Particle and trace element production from fires in the chaparral fuel type, *Paper No. 89-025.002, In: Proceedings of the 1989 National Air and Waste Management Association Meeting*, 1989 June 25-30; Anaheim, CA, Air and Waste Management Association: Pittsburgh, PA, 1989.

Hegg, D. A., L. F., Radke, P. V. Hobbs, R. A. Rasmussen, and P. J. Riggan, *Emissions of some trace gases from biomass fires, Distributed at 82nd APCA Annual Meeting, Anaheim, CA, June 25-30*, 13 pp, 1989.

McRae, D., Data presented at joint review meeting in Missoula, MT October 1989, *The effects on the atmosphere of a major nuclear exchange. On file Forestry Canada, Saulte Ste. Marie, Ontario, Canada.*

Perry, R. H. and C. H. Chilton, *Chemical Engineer's Handbook*, 5th edition, 3-145, McGraw-Hill, New York, 1973.

Radke, L. F., J. H. Lyons, D. A. Hegg, D. V. Sandberg, and D. E. Ward, Airborne monitoring and smoke characterization of prescribed fires on forest lands in western Washington and Oregon, U.S. Department of Agriculture, Forest Service, Pacific Northwest Research Station, Portland, OR, in press, 1990.

Rothermel, R. C., A mathematical model for predicting fire spread in wildland fuels, *Res. Pap. INT-115*, Ogden, UT: U.S. Department of Agriculture, Forest Service, Intermountain Forest and Range Experiment Station. 40 pp, 1972.

Rothermel, R. C., How to predict the spread and intensity of forest and range fires, *Gen. Tech. Rep. INT-143*, Ogden, UT: U.S. Department of Agriculture, Forest Service, Intermountain Forest and Range Experiment Station. 161 pp, 1983.

Ward, D. E. and C. C. Hardy, Advances in the characterization and control of emissions from prescribed fires, *Paper No. 84-36.3, In: Proceedings of the 78th annual meeting of the Air Pollution Control Association*; 1984 June 24-29; San Francisco, CA, Air Pollution Control Association, Pittsburgh, PA, 1984.

Ward, D. E. and C. C. Hardy, Emissions from prescribed burning of chaparral, In: *Proceedings 1989 Annual Meeting of the Air and Waste Management Association*, Anaheim, CA. in June '89. 22 pp, 1989.

Ward, D. E. and C. C. Hardy, Smoke Emissions from Wildland Fires. *Environment International*, *17*, 117-134, 1990.

Ward, D. E., R. M. Nelson, and D. F. Adams, Forest Fire Smoke Plume Documentation. In: *Proceedings of the 72nd Annual Meeting of the Air Pollution Control Association*, Cincinnati, OH. June 24-29, 1979. 24 pp, 1979.